Publication Year	2018
Acceptance in OA@INAF	2020-10-12T09:36:07Z
Title	Effective temperatures of red giants in the APOKASC catalogue and the mixing length calibration in stellar models
Authors	Salaris, M.; CASSISI, Santi; Schiavon, R. P.; PIETRINFERNI, Adriano
DOI	10.1051/0004-6361/201732340
Handle	http://hdl.handle.net/20.500.12386/27695
Journal	ASTRONOMY & ASTROPHYSICS
Number	612

Astronomy & Astrophysics manuscript no. RGBTeff˙postref
January 2, 2018
© ESO 2018

The effective temperatures of red giants in the APOKASC catalogue and the mixing length calibration in stellar models

M. Salaris[1], S. Cassisi[2], R. P. Schiavon[1], and A. Pietrinferni[2]

[1] Astrophysics Research Institute, Liverpool John Moores University, IC2, Liverpool Science Park, 146 Brownlow Hill, Liverpool, L3 5RF, UK (M.Salaris@ljmu.ac.uk)
[2] INAF-Osservatorio Astronomico d'Abruzzo, via M. Maggini, sn. 64100, Teramo, Italy

Received ; accepted

ABSTRACT

Red giants in the updated APOGEE-*Kepler* catalogue, with estimates of mass, chemical composition, surface gravity and effective temperature, have recently challenged stellar models computed under the standard assumption of solar calibrated mixing length. In this work, we critically reanalyse this sample of red giants, adopting our own stellar model calculations. Contrary to previous results, we find that the disagreement between the T_{eff} scale of red giants and models with solar calibrated mixing length disappears when considering our models and the APOGEE-*Kepler* stars with scaled solar metal distribution. However, a discrepancy shows up when α-enhanced stars are included in the sample. We have found that assuming mass, chemical composition and effective temperature scale of the APOGEE-*Kepler* catalogue, stellar models generally underpredict the change of temperature of red giants caused by α-element enhancements at fixed [Fe/H]. A second important conclusion is that the choice of the outer boundary conditions employed in model calculations is critical. Effective temperature differences (metallicity dependent) between models with solar calibrated mixing length and observations may appear for some choices of the boundary conditions, but this is not a general result.

Key words. convection – stars: low mass – stars: fundamental parameters

1. Introduction

Calculations of the superadiabatic convective temperature gradients in stellar evolution models are almost universally based on the very simple, local formalism provided by the mixing length theory (MLT – Böhm-Vitense 1958). The convective flow is idealized in terms of columns of upward and downward moving elements all with the same characteristic size, that cover a fixed mean free path before dissolving. Both the mean free path and the characteristic size of the convective elements are assumed to be equal to $\Lambda = \alpha_{\rm MLT} H_P$, the mixing length. The free parameter $\alpha_{\rm MLT}$ is typically assumed to be a constant value within the convective regions and along all evolutionary phases, and H_p is the local pressure scale height.

It is well known that this simplistic MLT picture of convection is very different from results of two-dimensional (2D) and three-dimensional (3D) radiation hydrodynamics simulations of convection in stellar envelopes/atmospheres (see, e.g., Stein & Nordlund 1989; Ludwig et al. 1999; Trampedach et al. 2014; Magic et al. 2015, and references therein). These computations show how convection consists mainly of continuous flows, with the warm gas rising almost adiabatically, in a background of cool, narrower and faster downdrafts. A fraction of the upflows is continuously overturning to conserve mass on the background of the steep density gradients.

We cannot obviously expect the MLT to provide an accurate description of the thermal stratification within the superadiabatic layers of convective envelopes, but only an *effective* **stratification that leads to an appropriate effective temperature (T_{eff}) scale for the stellar models. It is the chosen value of $\alpha_{\rm MLT}$ that determines the model T_{eff},** and this free parameter is usually calibrated by reproducing the radius of the Sun at the solar age with an evolutionary solar model (Gough & Weiss 1976). **Of course there is no reason** *a priori* **why $\alpha_{\rm MLT}$ should be the same with varying mass/evolutionary phase/chemical composition.**

Additional free parameters appear in the MLT formalism, but they are generally fixed beforehand, giving origin to different *flavours* of the MLT formalism (see, e.g., Pedersen et al. 1990; Salaris & Cassisi 2008, and references therein). Remarkably, different MLT flavours found in the literature provide essentially the same evolutionary tracks when α_{MLT} is accordingly recalibrated on the Sun (Pedersen et al. 1990; Salaris & Cassisi 2008).

One independent empirical way to calibrate and/or test whether the solar calibration of $\alpha_{\rm MLT}$ is appropriate also for other evolutionary phases/chemical compositions, is to compare empirically determined effective temperatures of red giant branch (RGB) stars, with theoretical models of the appropriate chemical composition, that are indeed very sensitive to the treatment of the superadiabatic layers (see,.e.g. Straniero & Chieffi 1991; Salaris & Cassisi 1996; Vandenberg et al. 1996, and references therein).

A very recent study by Tayar et al. (2017) has analyzed a sample of over 3000 RGB stars with T_{eff}, mass, surface gravity (g), [Fe/H] and [α/Fe] determinations from the updated APOGEE-*Kepler* catalogue (APOKASC), suited for testing the mixing length calibration in theoretical stellar models. According to the grid of stellar evolution models specifically calculated to match the T_{eff} values of the individual stars, this study (hereafter T17) concluded that a variation of $\alpha_{\rm MLT}$ with varying [Fe/H] is required. Their stellar models with solar calibrated α_{MLT} (the solar α_{MLT} in their calculations is equal to 1.72 when employing the Böhm-Vitense 1958, MLT flavour) are unable to match the empirical T_{eff} values for [Fe/H] between $\sim$ +0.4 and

−1.0. They calculated differences $\Delta T \equiv T_{obs} - T_{models}$ between observed and theoretical T_{eff} for each individual star in their sample, and found that ΔT=93.1[Fe/H]+ 107.5 K. They concluded that a varying mixing length $\alpha_{MLT} = 0.161[Fe/H] + 1.90$ is required to match the empirical temperatures. This relationship predicts a non solar α_{MLT} also for RGB stars at solar metallicity. The same authors found a similar trend of ΔT with [Fe/H] (a ΔT-[Fe/H] slope of about 100 K/dex) when using the PARSEC stellar models (Bressan et al. 2012), albeit with a zero point offset of about −100 K compared to the results obtained with their models.

A variation of α_{MLT} with [Fe/H] –and potentially with evolutionary phase– has obviously profound implications for the calibration of convection in stellar models, age estimates of RGB stars in the Hertzsprung-Russell and g-T_{eff} diagrams, and also stellar population integrated spectral features sensitive to the presence of a RGB component.

In light of the relevant implications of T17 result, we have reanalyzed their APOKASC sample with our own independent stellar evolution calculations, paying particular attention to the role played by uncertanties in the calculation of the model boundary conditions. Our new results clarify the role played by the combination of $\alpha_{\rm MLT}$ and boundary conditions in the interpretations of the data, and, very importantly, discloses also a major difficulty when comparing models with T17 α-enhanced stars.

Section 2 briefly summarizes T17 data and the models calculated for this work, followed in Sect. 3 by a description of our analysis and our new results. A summary and in-depth discussion of our findings closes the paper.

2. Models and data

For our analysis we have calculated a large set of models using code and physics inputs employed to create the BaSTI database of stellar evolution models (see Pietrinferni et al. 2004). **Because of the relevance to this work, we specify that radiative opacities are from the OPAL calculations (Iglesias & Rogers 1996) for temperatures larger than** log(T) = 4.0**, whereas calculations by Ferguson et al. (2005) –that include the contributions from molecules and grains– have been adopted for lower temperatures. Both high- and low-temperature opacity tables account properly for the metal distributions adopted in our models (see below and Sect. 3.2).**

We have just changed the $T(\tau)$ relation adopted in BaSTI to determine the models' outer boundary conditions (a crucial input for the determination of the models' T_{eff}, as discussed in Sect. 3.3), employing the Vernazza et al. (1981) solar semi-empirical $T(\tau)$ (hereafter VAL) instead of the Krishna Swamy (1966) one.[1].

According to the analysis by Salaris & Cassisi (2015), model tracks computed with this $T(\tau)$ relation approximate well results obtained using the hydro-calibrated $T(\tau)$ relationships provided by Trampedach et al. (2014) for the solar chemical composition. We will come back to this issue in Sect. 3.3.

We have computed a model grid for masses between 0.7 and 2.6 $M_{\odot}$ in 0.1 $M_{\odot}$ increments, and scaled solar [Fe/H] between −2.0 and +0.4 dex in steps of 0.2-0.3 dex. A solar model including atomic diffusion has been calibrated to determine initial solar values of He and metal mass fractions Y=0.274, Z=0.0199 (for the Grevesse & Noels 1993, solar metal mixture), and mixing length (with the MLT flavour from Böhm-Vitense 1958) $\alpha_{\rm MLT}$=1.90. We have adopted the same Y-Z relationship Y=0.245+1.41 $\times Z$ as in BaSTI. Our model grid does not include atomic diffusion, because its effect on the RGB evolution is, as well known, negligible (Salaris & Cassisi 2015). In addition, we have calculated sets of α-enhanced models for the various masses and [Fe/H] of the grid, and [α/Fe]=0.4.

[1] We implement the following fit to Vernazza et al. (1981) tabulation: $T^4 = 0.75\ T^4_{eff}\ (\tau + 1.017 - 0.3e^{-2.54\tau} - 0.291e^{-30\tau})$, where τ is the Rosseland optical depth

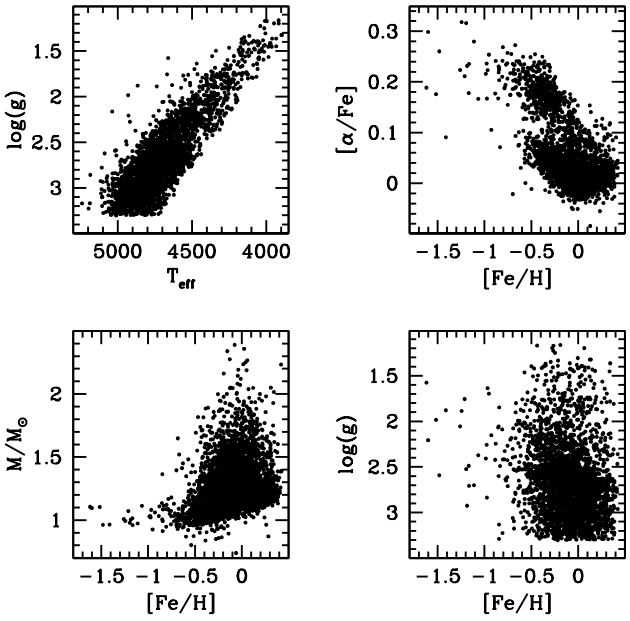

Fig. 1. The sample of RGB stars from the APOKASC dataset displayed in various diagrams: log(g) − T_{eff}, [α/Fe] − [Fe/H], mass − [Fe/H] and log(g) − [Fe/H].

With these models we have first reanalyzed the sample of RGB field stars by T17, considering the log(g), T_{eff}, [Fe/H] and [α/Fe] values listed in the publicly available data file. Masses are derived from asteroseismic scaling relations, and the other quantities are obtained using the APOGEE spectroscopic data set. The T_{eff} values are calibrated to be consistent with the González Hernández & Bonifacio (2009) effective temperature scale, based on the infrared-flux method.

We considered only the stars with a calculated error bar on the mass determinations (we excluded objects with error on the mass given as -9999), that still leave a sample of well over 3000 objects, spanning a mass range between 0.8 and 2.4 $M_{\odot}$, with a strong peak of the mass distribution around 1.2-1.3$M_{\odot}$.

Figure 1 displays the data in four different diagrams. The stars cover a log(g) range between ∼3.3 and 1.1 (in cgs units), and T_{eff} between ∼5200 and 3900 K, with the bulk of the stars having [Fe/H] between ∼ −0.7 and ∼ +0.4 dex, and a maximum α-enhancement typically around 0.25 dex. Notice that stars with a given [Fe/H] typically cover the full range of surface gravities, but the range of masses at a given [Fe/H] varies with metallicity, due to the variation of the age distribution of Galactic disk stars with [Fe/H].

To determine differences $\Delta T \equiv T_{obs} - T_{models}$ between observed and theoretical T_{eff} for each individual star in T17 sample, we have interpolated linearly in mass, [Fe/H], [α/Fe], log(g) amongst the models, to determine the corresponding theoretical T_{eff} for each observed star.

Table 1. Mean values of the differences ΔT (third column) for the full T17 sample, determined in [Fe/H] bins centred around the values given in the first column of the table, and half-widths listed in the second column. The last column displays the 1σ dispersion around the mean ΔT values.

[Fe/H]	$\pm\Delta[Fe/H]$	$<\Delta T>$ (K)	$\sigma(\Delta T)$ (K)
0.35	0.05	-35	24
0.25	0.05	-23	33
0.15	0.05	-21	31
0.05	0.05	-8	35
-0.05	0.05	-11	40
-0.15	0.05	-9	44
-0.25	0.05	-22	52
-0.35	0.05	-32	54
-0.45	0.05	-54	53
-0.60	0.10	-72	55

Table 2. As Table 1, but for stars with observed [α/Fe]<0.07.

[Fe/H]	$\pm\Delta[Fe/H]$	$<\Delta T>$ (K)	$\sigma(\Delta T)$ (K)
0.35	0.05	-34	23
0.25	0.05	-22	30
0.15	0.05	-18	29
0.05	0.05	-4	32
-0.05	0.05	-4	37
-0.15	0.05	0	39
-0.25	0.05	0	39
-0.35	0.05	-7	38
-0.45	0.05	-7	43
-0.60	0.10	-34	52

3. Analysis of T17 sample

The top panel of Fig. 2 displays the differences $\Delta T \equiv T_{obs} - T_{models}$ as a function of [Fe/H] for the full T17 sample; we have considered stars with [Fe/H]> −0.7, to include only the [Fe/H] range well sampled by the data.

It is easy to notice a trend of ΔT with [Fe/H], qualitatively similar to what found by T17. We have overplotted, as open circles, mean values of ΔT determined in ten [Fe/H] bins, with total width of 0.10 dex, apart from the most metal poor bin, that has a width of 0.20 dex, due to the smaller number of stars populating that metallicity range –see Table 1. The horizontal error bars cover the width of the individual bins, while the vertical ones denote the 1σ dispersion of ΔT around the mean values.

As in T17, we find a drop of ΔT with decreasing [Fe/H], when [Fe/H] is below ~ -0.25. If we perform a simple linear fit through these mean values (considering the 1σ dispersion as the *error* on these mean ΔT values) we obtain for the full sample ΔT=(39 ± 19) [Fe/H]−(25 ± 6) K, valid over a [Fe/H] range of ∼1.1 dex. A linear fit is clearly not the best approximation of the ΔT-[Fe/H] global trend –as mentioned also in T17– but it replicates T17 analysis and suffices to highlight the main results of these comparisons.

Our RGB models turn out to be systematically hotter than observations by just 25 K at solar [Fe/H], a negligible value considering the error on the González Hernández & Bonifacio (2009) T_{eff} calibration (the quoted average error on their RGB T_{eff} scale is ≤76 K), but the differences increase with decreasing [Fe/H]. The slope we derive is about half the value of the slope determined by T17 with their own calculations, and the zero point is about 130 K lower. We do not find any correlation between ΔT and the surface gravity g of the observed stars, as shown in Fig. 3.

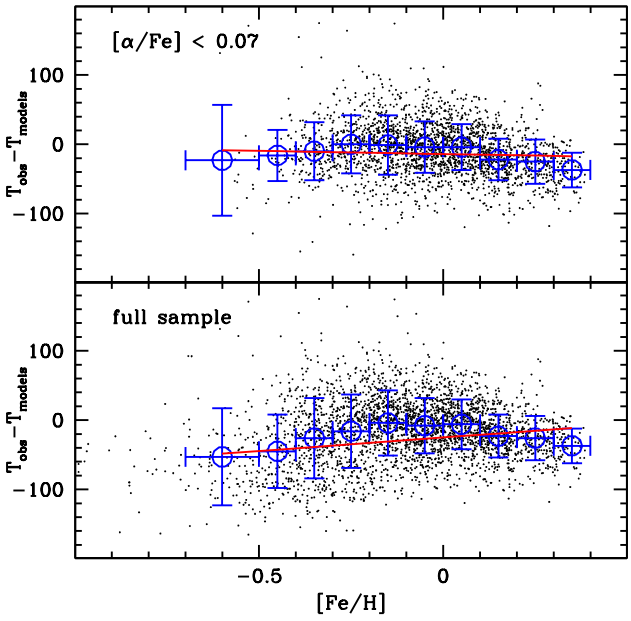

Fig. 2. ΔT as a function of [Fe/H] (dots) for the whole sample of RGB stars (bottom panel) and for a sub-sample of RGB objects with [α/Fe] < 0.07 (top panel). Open circles with error bars denote the mean values of ΔT in specific metallicity bins –columns 3 and 4 in Tables 1 and 2– while the solid lines display linear fits to the binned data.

The lower panel of Fig. 2 displays ΔT values considering this time only stars with essentially scaled solar metal mixture, i.e. [α/Fe]<0.07 (we chose this upper limit that is approximately equal to 5 times the 1σ error on [α/Fe] quoted in T17 data, but an upper limit closer to zero does not change the results). The overplotted mean values in the various [Fe/H] bins are reported in Table 2. This time the trend of ΔT with [Fe/H] is not statistically significant. A linear fit to the mean ΔT values provides ΔT=(−9 ± 15) [Fe/H]−(14 ± 5), meaning that now theory and observations are essentially in agreement.

Figure 4 makes clearer the reason for the different result obtained when neglecting the α-enhanced stars. We show here histograms of ΔT values for stars with [Fe/H] between −0.5 and −0.3, [α/Fe]<0.07 and [α/Fe]≥0.07, respectively. One can clearly see how, in the same [Fe/H] range, we determine for α-enhanced stars systematically lower ΔT values.

In conclusion, with our calculations the trend of ΔT with [Fe/H] is introduced by the inability of α-enhanced models with solar calibrated $\alpha_{\rm MLT}$ to match their observational counterparts, i.e. stellar models are increasingly hotter than observations when [α/Fe] increases, at fixed [Fe/H], even though we have taken into account the theoretically expected effect of [α/Fe] on the model T_{eff}, at a given [Fe/H]. Comparing the values in Tables 1 and 2 one can notice that the effect of excluding α-enhanced stars on the mean ΔT values appears around [Fe/H]=−0.25, consistent with the fact that below this [Fe/H] the fraction of α-enhanced stars increases, and [α/Fe] values also increase. On the other hand, and very importantly, our models with solar calibrated $\alpha_{\rm MLT}$ produce T_{eff} values for scaled solar stars that are generally consistent with observations over a [Fe/H] range of about 1 dex.

Our conclusions appear to be very different from T17 results obtained with their own model calculations, and therefore we have reanalyzed T17 temperature differences (with respect ot

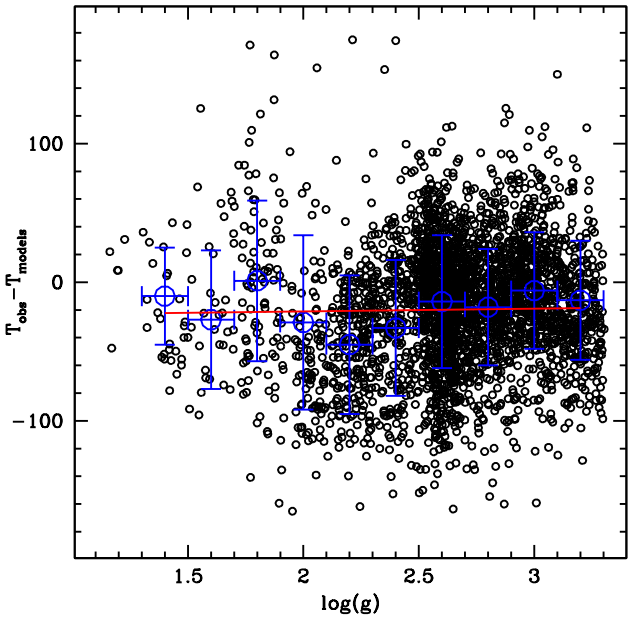

Fig. 3. ΔT as a function of log(g) for the whole sample of RGB stars. **Open circles with error bars denote the mean values of ΔT in 0.2 dex log(g) bins, and the 1σ dispersion around these mean values. The solid line displays a linear fit to the binned data, with a slope that is consistent with zero (the slope is equal to 2 ± 8 K/dex).**

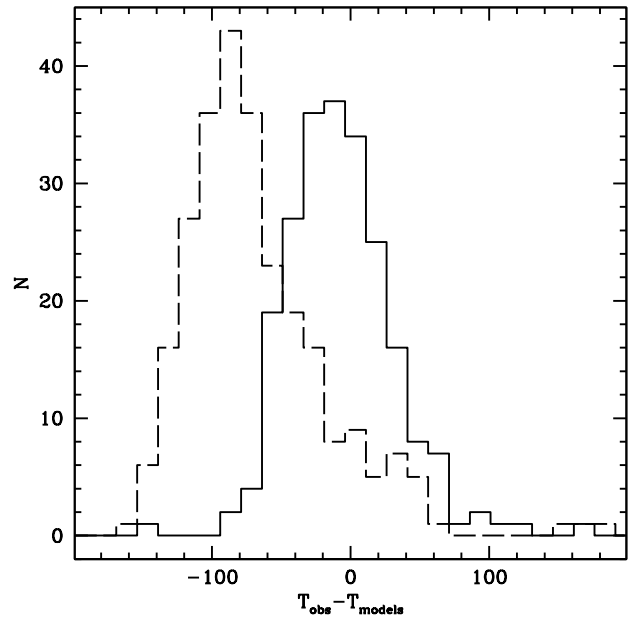

Fig. 4. Histograms ΔT for stars with [Fe/H] between −0.5 and −0.3, [α/Fe]< 0.07 (solid line) and [α/Fe]≥0.07 (dashed line)

their own solar calibrated $\alpha_{\rm MLT}$ models) on a star-by-star basis as provided by the authors[2], using exactly the same [Fe/H] bins discussed before. The results are displayed in Fig. 5. T17 ΔT values have been binned in the same [Fe/H] ranges employed for our own results, and we have then performed a linear fit to

[2] T17 did not provide the ΔT values they obtained employing the PARSEC models

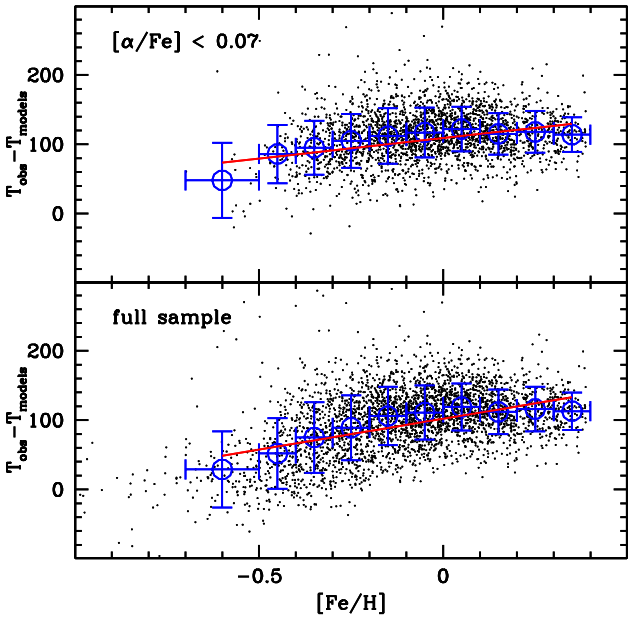

Fig. 5. As Fig. 2 but in this case individual ΔT values are from the study by T17.

the mean values of the ten [Fe/H] bins for both the full sample, and the sample restricted to stars with [α/Fe]<0.07.

The linear fit to the full sample provides ΔT=(89 ± 16) [Fe/H]+(102 ± 5) K. Slope and zero point are well consistent with the values (93.1 K/dex for the slope and 107.5 K for the zero point) determined by T17 using their different –finer– binning of the data. This means that the slight different way to analyze ΔT values as employed in our analysis, provides exactly the same results found by T17, when applied to T17 estimates of ΔT.

Restricting the sample to objects with [α/Fe]<0.07, the linear fit to T17 ΔT values provides ΔT=(59 ± 14) [Fe/H]+(109 ± 5) K. A slope different from zero is still present, contrary to what we find with our calculations, hence it cannot be attributed to just an *inconsistent* modelling of the α-enhanced population. On the other hand, this slope is lower than the case of the full sample, and implies that the match of α-enhanced stars with solar $\alpha_{\rm MLT}$ models increases the trend of ΔT with [Fe/H], compared to the case of just stars with scaled solar metal composition.

This is exemplified by Fig. 6, that is the same as Fig. 4, this time considering T17 ΔT values. One can see clearly that also in case of T17 models, α-enhanced stars at the same [Fe/H] display different (lower) ΔT compared to the scaled solar counterparts, exactly as in case of our models.

It is also important to notice also a large difference, of about 120 K, in the zero points compared to our results.

3.1. Revisiting the chemical composition of T17 stars

In light of the inconsistency between our solar calibrated $\alpha_{\rm MLT}$ models for α-enhanced compositions and the observed α-enhanced stars, we have investigated in more detail the chemical composition of T17 sample, looking at the abundances reported in the APOGEE DR13 catalogue (Majewski et al. 2017, and Holtzman et al., in preparation).

We have realized that [Fe/H] values reported by T17 are actually labelled as [M/H] in the DR13 catalogue, and [α/Fe] is ac-

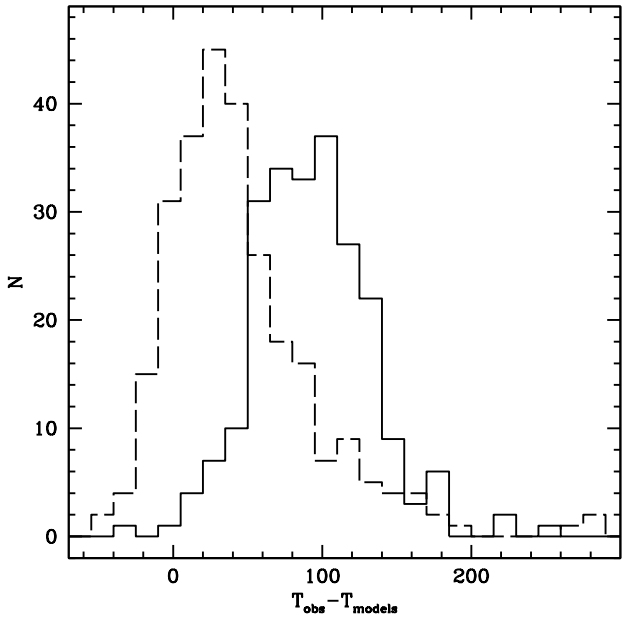

Fig. 6. As Fig. 4 but for the ΔT values from T17

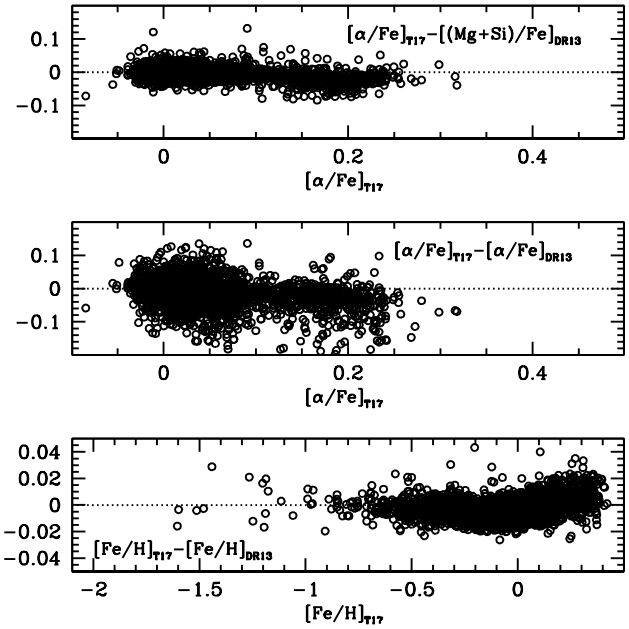

Fig. 7. *Bottom panel*: Difference between [Fe/H] values adopted by T17 ($[Fe/H]_{T17}$) and [Fe/H] as listed in the DR13 catalogue ($[Fe/H]_{D13}$), as a function of $[Fe/H]_{T17}$. *Middle panel*: Same as bottom panel, but for $[\alpha/Fe]$, considering the total α-enhancement from DR13 data (see text for details). *Top panel*: Same as middle panel, but in this case the DR13 estimate is actually [(Mg+Si)/Fe] (see text for details).

tually labelled as $[\alpha/M]$ in DR13. As explained in the APOGEE catalogue[3], the listed [M/H] is an overall scaling of metal abundances assuming a solar abundance ratio pattern, and $[\alpha/M]=[\alpha/H]-[M/H]_{\odot}$. This definition of [M/H] cannot be implemented in stellar evolution calculations in a straightforward fashion for α-enhanced metal mixtures, therefore we have extracted from the DR13 catalogue values for [Fe/H], and the listed α-element abundance ratios [O/Fe], [Mg/Fe], [Si/Fe], [Ca/Fe] and [Ti/Fe] for all stars in T17 sample.

The bottom panel of Fig. 7 compares these [Fe/H] values with the values listed by T17 (that correspond to [M/H] in DR13). The agreement is typically within ±0.02 dex, and suprisingly also for the α-enhanced stars. At any rate, the consequence is that the general agreement of the T_{eff} of our solar $\alpha_{\rm MLT}$ RGB models with the observed scaled solar metallicy stars is confirmed (as we have verified applying the preocedure described in the previous section, employing these DR13 [Fe/H] values) when using the DR13 values labelled as [Fe/H].

The top and middle panels of Fig. 7 compare the $[\alpha/Fe]$ values given by T17 (that correspond to $[\alpha/M]$ in DR13 catalogue) with two different estimates of $[\alpha/Fe]$ based upon the DR13 values of [O/Fe], [Mg/Fe], [Si/Fe], [Ca/Fe] and [Ti/Fe]. In the top panel we display our $[\alpha/Fe]$ values estimated as [(Mg+Si)/Fe], taking into account that Mg and Si are the two α-elements that affect the T_{eff} of RGB stellar evolution models (VandenBerg et al. 2012). We have calculated [(Mg+Si)/Fe] employing the observed [Mg/Fe] and [Si/Fe], and the Grevesse & Noels (1993) solar metal mixture used in the model calculations as a reference. The correspondence with $[\alpha/Fe]$ values listed by T17 (actually $[\alpha/M]$ in DR13) is remarkable, with an offset of typically just ∼0.01 dex when $[\alpha/Fe]>0.1$, and a very small spread.

The middle panel displays our $[\alpha/Fe]$ estimates accounting for all DR13 α-elements. On average our $[\alpha/Fe]$ tend to get systematically larger than T17 values , when $[\alpha/Fe]$ is larger than ∼0.1 dex, again by just 0.01-0.02 dex on average. However, there is now a large scatter (compared to the case of [(Mg+Si)/Fe]) in the differences. The reason for the different behaviour compared to the [(Mg+Si)/Fe] case is that the various α elements are not always enhanced by the same amount in the observed stars, hence the exact value of $[\alpha/Fe]$ to some degree depends on which elements are included in its definition.

From the point of view of testing the RGB model T_{eff}, what matters is that the chemical composition of the models match the observed [(Mg+Si)/Fe] (based on the results by VandenBerg et al. 2012). In case of the same enhancement for all α elements, typical of stellar evolution calculations, this means that the model $[\alpha/Fe]$ has to match the observed [(Mg+Si)/Fe]. Therefore the results of the comparison made in the previous section employing T17 $[\alpha/Fe]$ values still stand, given that T17 $[\alpha/Fe]$ corresponds very closely to [(Mg+Si)/Fe] as determined from the DR13 individual abundances.

Finally, Fig. 8 show very clearly the problem when matching the T_{eff} of α-enhanced stars with models. We have displayed the $\log(g)$-T_{eff} diagram of two samples of stars with observed mean mass equal to $1.1M_{\odot}$ and mean [Fe/H] equal −0.35 dex, one with $[\alpha/Fe]$ ([(Mg+Si)/Fe]) smaller than 0.07 dex (the scaled solar sample), the other one with average $[\alpha/Fe]=0.20$ (the α-enhanced sample) respectively. These two sets of stars are distributed along well separated sequences, the α-enhanced one being redder than the scaled solar sequence, as expected. The T_{eff} difference between the two sequences is about 110 K at fixed $\log(g)$.

We have also plotted $1.1M_{\odot}$, [Fe/H]−0.35 models both scaled solar and with $[\alpha/Fe]=0.4$, from our own calculations and from Dotter et al. (2008) isochrone database, for a comparison. For these latter models we have used the online webtool[4] and calculated [Fe/H]=−0.35 isochrones populated by $\sim 1.1_{\odot}$ stars along the RGB.

[3] http://www.sdss.org/dr12/irspec/aspcap/

[4] http://stellar.dartmouth.edu/models/webtools.html

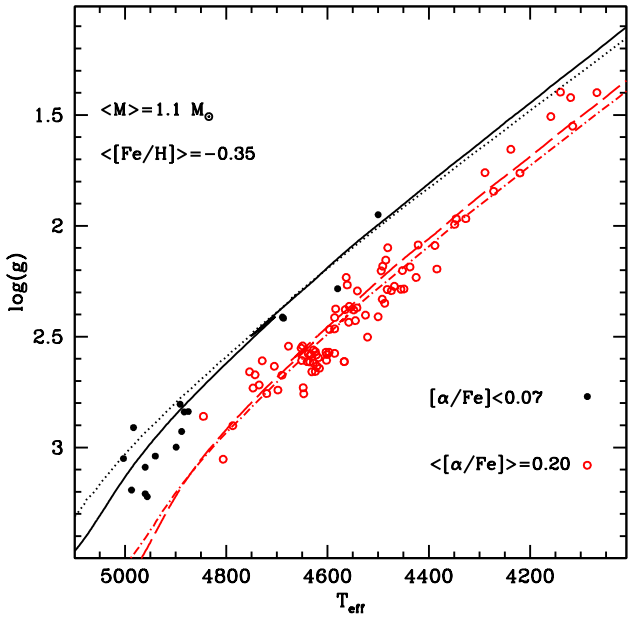

Fig. 8. log(g) − T_{eff} diagram of two sub-samples of APOKASC RGB stars with average [Fe/H] = −0.35 and mass 1.1M$_\odot$, but different α−enhancements: scaled solar objects ([α/Fe]<0.07, filled circles) and α−enhanced (average [α/Fe] = 0.2, open circles). Our 1.1M$_\odot$, [Fe/H]=−0.35 evolutionary tracks for [α/Fe] = 0 (solid line) and +0.40 (dashed line) are also displayed. The α-enhancement of the theoretical models is twice the average enhancement of the selected α-enhanced stars. Dotted and dot-dashed lines show tracks with the same mass, [Fe/H] and α-enhancements, from Dotter et al. (2008).

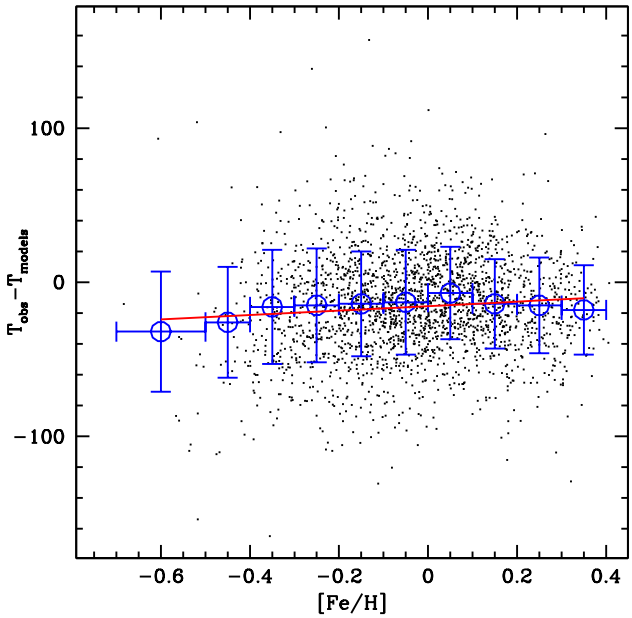

Fig. 9. ΔT as a function of [Fe/H] for the sub-sample of RGB objects with [α/Fe] < 0.07, using stellar models calculated with the Caffau et al. (2011) plus Lodders (2010) solar metal distribution (see text for details).

The observed T_{eff} difference between scaled solar and α-enhanced stars turns out to be reproduced by both independent sets of stellar models for [α/Fe]∼0.4, twice the observed value.

This further analysis confirms that the trend of ΔT with [Fe/H] obtained with our models is due to the fact that they are systematically hotter than observations for α-enhanced stars. Also, this discrepancy between α-enhanced RGB stellar models and observations seems to be more general, not just related to our models.

3.2. The effect of the solar metal distribution

To assess better the good agreement between our scaled solar models and RGB sample ([α/Fe]<0.07), we have also calculated a set of models with the same physics inputs but a more recent determination of the solar metal distribution (both opacities and equation of state take into account the new metal mixture), from Caffau et al. (2011) for the most abundant elements, complemented with abundances from Lodders (2010). We have covered the same range of masses and [Fe/H] of the reference models employed in the analysis described in the previous sections. Notice that T17 calculations use the Grevesse & Sauval (1998) solar metal distribution, very similar to the Grevesse & Noels (1993) one of our reference calculations.

The Caffau et al. (2011) solar metal mixture implies a lower metallicity for the Sun compared to Grevesse & Noels (1993)[5]. Our calibrated solar model provides an initial He abundance Y=0.269, metallicity Z=0.0172, $\alpha_{\rm MLT}$=2.0, and $\Delta Y/\delta Z$=1.31.

Figure 9 displays the ΔT values as a function of [Fe/H] for the scaled solar sample. **We have binned the ΔT values and performed a linear fit to the binned data as in Fig. 2, deriving a slope that is statistically consistent with zero** for [Fe/H] larger than ∼ −0.6 dex, that is, over a [Fe/H] range of about 1 dex. The average ΔT is equal to −14 K, with a 1σ dispersion of 34 K. We can conclude that changing the reference solar metal distribution and the corresponding solar calibrated $\alpha_{\rm MLT}$ does not alter the agreement between our models and the T_{eff} of the scaled solar T17 sample of RGB stars.

3.3. The effect of the model boundary conditions

As discussed in Kippenhahn et al. (2012), the outer boundary conditions for the solution of the stellar evolution equations have a major effect on models with deep convective envelopes, like the RGB ones. We have therefore explored in some detail this issue, to check whether different choices of how the boundary conditions are determined can cause metallicity dependent T_{eff} differences amongst models with the same total mass, and eventually –at least partially– explain the differences between our and T17 results.

The physics inputs of BaSTI and T17 calculations are very similar, the main difference being their integration of the Eddington grey $T(\tau)$ to determine the boundary conditions, whereas we used the VAL $T(\tau)$[6]. We have therefore investigated the role played by different $T(\tau)$ choices to determine the outer boundary conditions of our model calculations (see also, e.g. Montalbán et al. 2004; VandenBerg et al. 2008, for investigations

[5] The solar metallicity from the Caffau et al. (2011) determination is slightly higher than what would be obtained with the Asplund et al. (2009) solar metal mixture

[6] The equation of state (EOS) is also different (see T17 and Pietrinferni et al. 2004), but tests made by Pietrinferni et al. (2004) have shown that the EOS employed by T17 produces tracks very close to the ones obtained with the BaSTI EOS choice

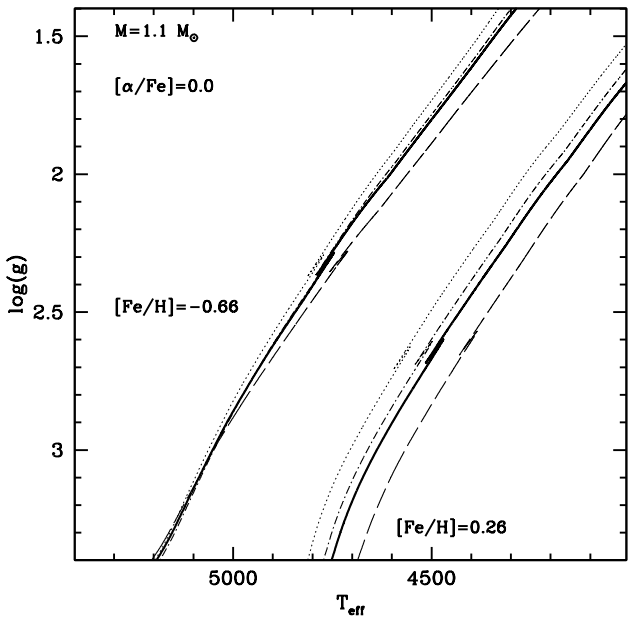

Fig. 10. Scaled solar evolutionary tracks for the labelled mass and [Fe/H] values. The tracks correspond to models calculated with the KS (dotted lines), VAL (solid lines), HM (dash-dotted lines) and EDD (dashed lines) $T(\tau)$ relationships, respectively (see text for details).

of the effect of boundary conditions on the T_{eff} of low-mass stellar models with convective envelopes), when comparing theory with the measured T_{eff} of T17 sample.

Figure 10 displays two groups of four RGB tracks in the T_{eff}-log(g) diagram (within the T_{eff} and log(g) range sampled by T17 data), for 1.1$M_{\odot}$ models with the labelled [Fe/H] (scaled solar metal mixtures). The two chosen [Fe/H] values bracket the metallicity range covered by our ΔT-[Fe/H] analysis, and the four tracks for each [Fe/H] represent four different choices for the $T(\tau)$ relation used to determine the outer boundary conditions.

Our reference calculations employing the VAL $T(\tau)$ are plotted together with calculations using an Eddington grey $T(\tau)$ (hereafter EDD) like T17 models, the Krishna Swamy (1966) (hereafter KS) and the Holweger & Mueller (1974) (hereafter HM) one[7]. The KS and HM $T(\tau)$ relationships are also solar semi-empirical, like the VAL $T(\tau)$.

Values of $\alpha_{\rm MLT}$ for these additional models have been fixed again by means of a solar calibration, and are equal to 1.70 (very close to the value 1.72 determined by T17 with their own calculations) 2.11 and 1.99 for calculations with the EDD, KS and HM $T(\tau)$, respectively. For the sake of comparison, we remind the reader that the solar calibration with the VAL $T(\tau)$ requires $\alpha_{\rm MLT}$ = 1.90/

It is striking not only that different $T(\tau)$ relations and their corresponding solar calibrated $\alpha_{\rm MLT}$ values produce RGBs with different T_{eff} (this was already shown for example in Salaris et al. 2002), but also that differences depend on the model [Fe/H]. These results are qualitatively and quantitatively the same also for masses equal to 2.0-2.5 $M_{\odot}$, at the upper end of the mass range spanned by T17 data. Clearly, different solar calibrations of $\alpha_{\rm MLT}$ obtained with different $T(\tau)$ relations do not guarantee consistent behaviours of RGB models with metallicity.

At [Fe/H]=+0.26, all tracks are roughly parallel. The EDD track is cooler by ∼70 K compared to the reference VAL one, whereas the KS track is hotter by about the same amount, and the HM track is hotter by just ∼25 K. At solar metallicity (not shown in the figure) the differences between EDD, VAL, KS and HM tracks are still about the same as at [Fe/H]=+0.26, whilst at [Fe/H]=−0.66 EDD, VAL and KS tracks are no longer parallel. Above log(g)∼2.8 they are roughly coincident, with T_{eff} differences increasing with decreasing log(g). At log(g)=1.5 the EDD track is cooler by ∼40 K, while the KS track is hotter by ∼30 K. The HM track is almost coincident with the VAL one.

We have seen before that ΔT values determined from our calculations employing the VAL $T(\tau)$ relation do not show any trend with T_{eff}, and are consistent with zero when scaled solar stars are considered. Employing instead the EDD $T(\tau)$ would increase ΔT values by ∼70 K at the upper end of the sampled [Fe/H] range down to about solar (EDD tracks being systematically cooler than VAL tracks), whilst the increase ranges from negligible to at most 40 K (when gravity decreases) at the lowest end of the [Fe/H] range considered in our analysis. This would induce an overall positive trend in the ΔT-[Fe/H] diagram (ΔT decreasing with decreasing [Fe/H]) also when restricting the analysis to scaled solar objects, with absolute ΔT values generally positive. This is at least qualitatively consistent with T17 results, even though it does not fully explain quantitatively T17 results, especially the very large positive ΔT at solar metallicity. Notice that also the PARSEC calculations –that according to T17 study show also a ΔT-[Fe/H] slope of about 100 K/dex– employ an Eddington grey $T(\tau)$ relationship to determine the model outer boundary conditions.

Finally, we is also interesting to notice that Dotter et al. (2008) models display T_{eff} values very close to ours over the whole mass, surface gravity and [Fe/H] range covered by our analysis (see also Fig. 8). In those models the boundary conditions have been taken from a grid of PHOENIX detailed 1D model atmospheres (pressure and temperature at a given optical depth τ, see Dotter et al. 2008) instead of a $T(\tau)$ integration.

4. Summary and discussion

Our reanalysis of the T17 sample of RGB stars from the APOKASC catalogue has disclosed the following:

1. According to the APOKASC T_{eff}, log(g), mass, [Fe/H] and [α/Fe] values given by T17, theoretical stellar evolution calculations –both our own calculations and T17 models, and also Dotter et al. (2008) calculations– seem to underestimate the effect of α-enhancement on the model T_{eff} at fixed mass, surface gravity and [Fe/H].
2. When α-enhanced stars are neglected, our RGB models are in good agreement with the empirical T_{eff} values, with no significant systematic shifts, nor trends with [Fe/H], over a ∼1 dex [Fe/H] range ([Fe/H] between ∼ +0.4 and ∼ −0.6). This agreement is preserved also if we change the reference solar metal distribution of our models.
3. For a solar calibrated $\alpha_{\rm MLT}$, the T_{eff} differences between theory and observations depend on the choice of the model boundary conditions. It is the combinations of boundary conditions and $\alpha_{\rm MLT}$ value that determine the T_{eff} of RGB stellar models, as expected for stars with deep convective envelopes (Kippenhahn et al. 2012).

[7] We employed the analytical fit by Vandenberg & Poll (1989) to the Holweger & Mueller (1974) data

Regarding the discrepancy between our models and α-enhanced stars, a variation of $\alpha_{\rm MLT}$ with [α/Fe] at a given [Fe/H] seems unlikely –but of course cannot be *a-priori* dismissed. Another possibility that we have checked is the role played by the $\Delta Y/\Delta Z$ enrichment ratio used in the model calculations. This value is typically fixed by the assumed primordial He and the solar initial Y (and Z) obtained from a standard solar model. For a fixed value of [Fe/H], α-enhanced stars have a larger Z, hence the corresponding models will have been calculated with a larger Y compared to the scaled solar counterparts at the same [Fe/H] (see, e.g., Table 3 in Dotter et al. 2008). What if the initial Y of α-enhanced stars is the same as for the scaled solar ones at a given [Fe/H]? In the [Fe/H] range of T17 stars and for the observed α-enhancements, the initial Y of the α-enhanced models will be at most ∼0.01 larger at the same [Fe/H], according to the $\Delta Y/\Delta Z$ value used in our calculations. This small variation of Y increases the T_{eff} of the models by ∼20 K in the relevant g range, hence our α-enhanced models would be at most 20 K cooler at fixed [Fe/H], if Y is the same as for the scaled solar stars. Such a small change of the model T_{eff} would not erase the discrepancy with observations.

From the empirical point of view, assuming metal abundance, g and T_{eff} scales are correct, asteroseismic masses systematically too high by 0.1-0.2 $M_{\odot}$ for α-enhanced stars could explain the discrepancy. Another possibility – assuming mass, g and T_{eff} values are correct– is that [Fe/H] determinations are too low by ∼0.1 dex for each 0.1 dex of α-enhancement, or a combination of both mass and [Fe/H] systematic errors. Of course it is necessary also to investigate this problem with stellar evolution models, to see whether there is room to explain this discrepancy from the theoretical side.

Concerning possible mixing length variations with chemical composition, we conclude that to match T17 T_{eff} values for the scaled solar subsample, variations of $\alpha_{\rm MLT}$ with [Fe/H] are required only for some choices of the model outer boundary conditions. Depending on the chosen $T(\tau)$ relation, or more in general the chosen set of boundary conditions, a variation of $\alpha_{\rm MLT}$ with [Fe/H] may or may not be necessary. Trying to determine whether $\alpha_{\rm MLT}$ can be assumed constant irrespective of chemical composition (and mass) for RGB stars thus requires a definitive assessment of the most correct way to determine the model outer boundary conditions.

As a consequence, models calculated with $\alpha_{\rm MLT}$ calibrations based on 3D radiation hydrodynamics simulations (Trampedach et al. 2014; Magic et al. 2015) are physically consistent only when boundary conditions (and physics inputs) extracted from the same simulations are employed in the stellar model calculations. We have achieved this consistency in Salaris & Cassisi (2015), testing the impact of Trampedach et al. (2014) simulations on stellar modelling.

Salaris & Cassisi (2015) have shown that at solar metallicity –the single metallicity covered by these 3D calculations– RGB models calculated with the hydro-calibrated variable $\alpha_{\rm MLT}$ (that is a function of T_{eff} and $\log(g)$) are consistent –within about 20 K– with RGB tracks obtained with the solar $\alpha_{\rm MLT}$ derived from the same set of hydro-simulations. They also found that the VAL $T(\tau)$ relationship provides RGB effective temperatures that agree quite well with results obtained with the hydro-calibrated $T(\tau)$ relationship, within typically 10 K. Assuming these hydro-simulations are realistic and accurate, the use of the VAL $T(\tau)$ and solar calibrated $\alpha_{\rm MLT}$ seems to be adequate for RGB stars at solar [Fe/H].

The independent 3D hydro-simulations by Magic et al. (2015) cover a large [Fe/H] range, from −4.0 to +0.5, and provide corresponding calibrations of $\alpha_{\rm MLT}$ in terms of [Fe/H], T_{eff}, and $\log(g)$. However, $T(\tau)$ relationships (or tables of boundary conditions) obtained from their simulations, plus Rosseland mean opacities consistent with the opacities used in their calculations, are not yet available, This means that their $\alpha_{\rm MLT}$ calibration cannot be consistently implemented in stellar evolution calculations yet, and one cannot yet check consistently whether the variable $\alpha_{\rm MLT}$ provides RGB T_{eff} values significantly different from the case a solar hydro-calibrated $\alpha_{\rm MLT}$ for the full range of [Fe/H] covered by these simulations.

Acknowledgements. SC acknowledges financial support from PRIN-INAF2014 (PI: S. Cassisi) and the Economy and Competitiveness Ministry of the Kingdom of Spain (grant AYA2013-42781-P).

References

Asplund, M., Grevesse, N., Sauval, A. J., & Scott, P. 2009, ARA&A, 47, 481
Böhm-Vitense, E. 1958, ZAp, 46, 108
Bressan, A., Marigo, P., Girardi, L., et al. 2012, MNRAS, 427, 127
Caffau, E., Ludwig, H.-G., Steffen, M., Freytag, B., & Bonifacio, P. 2011, Sol. Phys., 268, 255
Dotter, A., Chaboyer, B., Jevremović, D., et al. 2008, ApJS, 178, 89
Ferguson, J. W., Alexander, D. R., Allard, F., et al. 2005, ApJ, 623, 585
González Hernández, J. I. & Bonifacio, P. 2009, A&A, 497, 497
Gough, D. O. & Weiss, N. O. 1976, MNRAS, 176, 589
Grevesse, N. & Noels, A. 1993, Physica Scripta Volume T, 47, 133
Grevesse, N. & Sauval, A. J. 1998, Space Sci. Rev., 85, 161
Holweger, H. & Mueller, E. A. 1974, Sol. Phys., 39, 19
Iglesias, C. A. & Rogers, F. J. 1996, ApJ, 464, 943
Kippenhahn, R., Weigert, A., & Weiss, A. 2012, Stellar Structure and Evolution
Krishna Swamy, K. S. 1966, ApJ, 145, 174
Lodders, K. 2010, Astrophysics and Space Science Proceedings, 16, 379
Ludwig, H.-G., Freytag, B., & Steffen, M. 1999, A&A, 346, 111
Magic, Z., Weiss, A., & Asplund, M. 2015, A&A, 573, A89
Majewski, S. R., Schiavon, R. P., Frinchaboy, P. M., et al. 2017, AJ, 154, 94
Montalbán, J., D'Antona, F., Kupka, F., & Heiter, U. 2004, A&A, 416, 1081
Pedersen, B. B., Vandenberg, D. A., & Irwin, A. W. 1990, ApJ, 352, 279
Pietrinferni, A., Cassisi, S., Salaris, M., & Castelli, F. 2004, ApJ, 612, 168
Salaris, M. & Cassisi, S. 1996, A&A, 305, 858
Salaris, M. & Cassisi, S. 2008, A&A, 487, 1075
Salaris, M. & Cassisi, S. 2015, A&A, 577, A60
Salaris, M., Cassisi, S., & Weiss, A. 2002, PASP, 114, 375
Stein, R. F. & Nordlund, A. 1989, ApJ, 342, L95
Straniero, O. & Chieffi, A. 1991, ApJS, 76, 525
Tayar, J., Somers, G., Pinsonneault, M. H., et al. 2017, ApJ, 840, 17
Trampedach, R., Stein, R. F., Christensen-Dalsgaard, J., Nordlund, Å., & Asplund, M. 2014, MNRAS, 445, 4366
VandenBerg, D. A., Bergbusch, P. A., Dotter, A., et al. 2012, ApJ, 755, 15
Vandenberg, D. A., Bolte, M., & Stetson, P. B. 1996, ARA&A, 34, 461
VandenBerg, D. A., Edvardsson, B., Eriksson, K., & Gustafsson, B. 2008, ApJ, 675, 746
Vandenberg, D. A. & Poll, H. E. 1989, AJ, 98, 1451
Vernazza, J. E., Avrett, E. H., & Loeser, R. 1981, ApJS, 45, 635